Sensorless Control of Permanent Magnet Synchronous Motor Based on New Sliding Mode Observer with Single Resistor Current Reconstruction

Qingguo Sun, *Member, IEEE,* Xiaolei Zhu, and Feng Niu, *Member, IEEE*

***Abstract*—To solve the chattering problem caused by discontinuous switching function in traditional sliding mode observer, a piecewise square root switching function with continuously varying characteristics is designed, and its stability is analyzed by using Lyapunov stability criterion. Secondly, according to the relationship among bus current, switching state and phase current, a single bus resistance sampling current reconstruction scheme without current sensors is adopted, which effectively reduces the cost of motor system. Finally, the feasibility and effectiveness of the proposed scheme are verified by simulation.**

***Index Terms*—Permanent magnet synchronous motor, New sliding mode observer, Phase-locked loop, Single resistor, Current reconstruction.**

I. Introduction

PERMANENT magnet synchronous motor (PMSM) has been widely concerned and applied in aerospace, electric vehicles and other fields because of its simple structure, small size, light weight, high efficiency, high power density and so on[1]. However, obtaining the rotor position by installing the position sensor will bring the increase of cost, the decrease of reliability and the limitation of application. Therefore, sensorless control has become the current research hotspot[2]. sliding mode observer (SMO) technology has the characteristics of simple design, strong robustness and insensitive to the change of parameters, so it has become a potential position sensorless control scheme for medium and high speed PMSM[3].

The switch signal is usually used to modify the back electromotive force (EMF) of the constructed motor system based on sliding mode observer. Then the speed and position are obtained by back EMF. However, in the traditional sliding mode observer, the sliding mode function in the form of switch is used for position estimation, its inherent discontinuous switching characteristics and the electromagnetic parameter noise introduced by the motor system cause system chattering, which seriously affects the accuracy of position estimation[4]. In order to weaken the chattering phenomenon, smooth saturation function, sigmoid function, piecewise exponential function and hyperdistortion function are respectively adopted in [5]-[8], and make use of their continuous variation characteristics to make the approaching process of the system smoother, so that the sliding mode observer can run at a lower speed. The sinusoidal switching function which accords with the characteristics of back EMF is introduced in [9] to avoid the complex operation of exponential function. Furthermore, in order to improve the convergence of sinusoidal switching function, a sinusoidal saturation function with variable boundary layer is proposed in [10], which not only achieves fast convergence but also ensures the estimation accuracy. In addition, the chattering of the system can be suppressed by optimizing the sliding mode approach rate[11], designing a new filter[12] and adjusting the sliding mode gain[13].

In order to further reduce the cost of the motor control system, a single bus current sensor is used to obtain bus current and reconstruct three-phase current in [14], which reduces the number of current sensors. And the single-bus current sensor is replaced by single-bus resistance in [15], which further saves the cost. The reference [16] realizes the current reconstruction in the over-modulation region by changing the installation position of the single current sensor, and avoids the current distortion by improving the traditional vector pulse insertion method, but the program is complicated.

A new switching function, piecewise square root function, is proposed to suppress sliding mode chattering in this paper, and the stability is determined by constructing Lyapunov equation. Meanwhile, in order to improve the accuracy and immunity of rotor position estimation, this paper uses phase-locked loop (PLL) for position estimation. In addition, in order to further reduce the system cost, a single bus resistance scheme which through sampling the voltage of bus resistance and combining the switching state to reconstruct the three-phase current is adopted in this paper. Finally, the feasibility and effectiveness of the above scheme are verified by simulation.

Manuscript received April 19, 2022; revised March 10, 2022; accepted March 14, 2022. date of publication December 25, 2022; date of current version December 18, 2022.

Qingguo Sun, Xiaolei Zhu, and Feng Niu are with Hebei University of Technology. (e-mail: qingguosun@hebut.edu.cn, lwsunqg@163.com; 202121401084@stu.hebut.edu.cn; niufeng@hebut.edu.cn)

(Corresponding Author: Qingguo Sun)

Digital Object Identifier 10.30941/CESTEMS.2022.00049

II. DESIGN OF A NEW SLIDING MODE OBSERVER

A. Construction of a new sliding mode observer

The mathematical model of the interior PMSM in the d-q rotating frame is given by

$$\begin{cases} \dfrac{di_d}{dt} = \dfrac{1}{L_d}(u_d - Ri_d + \omega_e L_q i_q - e_d) \\ \dfrac{di_q}{dt} = \dfrac{1}{L_q}(u_q - Ri_q - \omega_e L_d i_d - e_q) \\ e_d = 0 \\ e_q = \omega_e \psi_f \end{cases} \tag{1}$$

where i_d, i_q, u_d, u_q are stator currents and voltages in the d-q rotating frame respectively, R is the stator resistance, L_d, L_q are the inductors in the direct and quadrature axis respectively, ω_e is the electric angular velocity, e_d, e_q are the induced electromotive forces in the direct and quadrature axis respectively, ψ_f is the permanent magnet flux linkage.

According to the sliding mode variable structure control theory, the mathematical model of the traditional sliding mode observer is designed as

$$\begin{cases} \dfrac{d\hat{i}_d}{dt} = \dfrac{1}{L_d}(u_d - R\hat{i}_d + \omega_e L_q \hat{i}_q - K\,\text{sgn}(\hat{i}_d - i_d)) \\ \dfrac{d\hat{i}_q}{dt} = \dfrac{1}{L_q}(u_q - R\hat{i}_q - \omega_e L_d \hat{i}_d - K\,\text{sgn}(\hat{i}_q - i_q)) \end{cases} \tag{2}$$

where $\hat{i}_d$, $\hat{i}_q$ are stator estimated currents in the d-q rotating frame respectively, K is the sliding mode gain, sgn() is the symbolic function.

Subtracting (1) from (2), the state equation of stator current error can be expressed as

$$\begin{cases} \dfrac{d\tilde{i}_d}{dt} = \dfrac{1}{L_d}(-R\tilde{i}_d + \omega_e L_q \tilde{i}_q - K\,\text{sgn}(\hat{i}_d - i_d) + e_d) \\ \dfrac{d\tilde{i}_q}{dt} = \dfrac{1}{L_q}(-R\tilde{i}_q - \omega_e L_d \tilde{i}_d - K\,\text{sgn}(\hat{i}_q - i_q) + e_q) \end{cases} \tag{3}$$

where $\tilde{i}_d$, $\tilde{i}_q$ are the error between estimated value and actual value of stator current in the d-q rotating frame respectively.

Rewrite equation (3) into vector form as

$$\dot{\tilde{\boldsymbol{i}}} = \boldsymbol{T}\tilde{\boldsymbol{i}} + \boldsymbol{B}(-K\,\text{sgn}(\tilde{\boldsymbol{i}}) + \boldsymbol{e}) \tag{4}$$

where, $\tilde{\boldsymbol{i}} = \begin{bmatrix} \tilde{i}_d & \tilde{i}_q \end{bmatrix}^{\mathrm{T}}$; $\boldsymbol{e} = \begin{bmatrix} e_d & e_q \end{bmatrix}^{\mathrm{T}}$;

$$\boldsymbol{T} = \begin{bmatrix} -\dfrac{R}{L_d} & \dfrac{L_q}{L_d}\omega_e \\ -\dfrac{L_d}{L_q}\omega_e & -\dfrac{R}{L_q} \end{bmatrix};\ \boldsymbol{B} = \begin{bmatrix} \dfrac{1}{L_d} & 0 \\ 0 & \dfrac{1}{L_q} \end{bmatrix}.$$

Define the sliding surface of the system as

$$\boldsymbol{s} = \tilde{\boldsymbol{i}} \tag{5}$$

where $\boldsymbol{s} = \begin{bmatrix} \boldsymbol{s}_d & \boldsymbol{s}_q \end{bmatrix}^{\mathrm{T}}$.

In order to weaken the sliding mode chattering, a piecewise square root switching function is designed to replace the switching function as

$$f(x) = \begin{cases} 1 & x \ge a \\ \sqrt{\dfrac{x}{a}} & 0 \le x < a \\ -\sqrt{\dfrac{-x}{a}} & -a < x < 0 \\ -1 & x < -a \end{cases} \tag{6}$$

where x is the output of sliding surface function, a is the boundary layer thickness. The new switching function has the characteristics of continuous variation in the boundary layer and saturation outside the boundary layer, which can achieve a good buffeting weakening effect. Fig. 1 shows the new switching function.

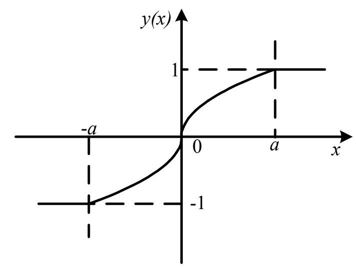

Fig. 1. A piecewise square root switching function.

The piecewise square root switching function proposed in this paper avoids the phenomenon that the change rate of the new piecewise exponential switching function in [7] is zero at zero. In addition, although the variation trend of the proposed function is similar to that of the sigmoid function in the boundary layer, it does not need complex exponential operation and is easier to implement.

Based on the proposed piecewise square root switching function, the new stator current error state equation can be rewritten as

$$\dot{\tilde{\boldsymbol{i}}} = \boldsymbol{T}\tilde{\boldsymbol{i}} + \boldsymbol{B}(-Kf(\boldsymbol{s}) + \boldsymbol{e}) \tag{7}$$

When the system reaches the sliding surface, it is satisfied

$$\boldsymbol{s} = \dot{\boldsymbol{s}} = 0 \tag{8}$$

where $\dot{\boldsymbol{s}}$ is the differential of $\boldsymbol{s}$.

According to (5), (7) and (8), the observed value of the back EMF can be written as

$$\begin{cases} Kf(s_d) = e_d = 0 \\ Kf(s_q) = e_q = \omega_e \psi_f \end{cases} \tag{9}$$

The traditional sliding mode observer has discontinuous switching state, so there must be discontinuous high-frequency signals in the EMF observations constructed by the traditional sliding mode observer. In order to obtain the accurate rotor position, it is generally necessary to filter the induced EMF observations which will cause rotor position estimation error. However, the new switching function proposed in this paper can not only effectively suppress the sliding mode chattering, but also effectively weaken the discontinuous high frequency signals in the induced EMF observations, thus avoiding the introduction of the filter. The estimation error caused by the use of low-pass filter in sliding mode observer is eliminated indirectly.

B. Stability analysis

In this paper, the stability of the new sliding mode observer is analyzed by Lyapunov stability criterion. Define the Lyapunov function as

$$V=\frac{1}{2}({s_d}^2+{s_q}^2) \tag{10}$$

Derive the equation (10) and make it satisfy the stability condition $\dot{V}\le 0$, so

$$\begin{aligned}\dot{V}&=s_d\dot{s}_d+s_q\dot{s}_q\\&=-\frac{R}{L_d}s_d^2+\frac{L_q}{L_d}\omega_e s_d s_q+\frac{s_d}{L_d}(-Kf(s_d)+e_d)\\&-\frac{R}{L_q}s_q^2-\frac{L_d}{L_q}\omega_e s_d s_q+\frac{s_q}{L_q}(-Kf(s_q)+e_q)\end{aligned} \tag{11}$$

Therefore, when the sliding mode gain is satisfied (12), the new sliding mode observer proposed in this paper satisfies the stability condition of Lyapunov stability criterion and can make the current error converge to zero in finite time.

$$K\ge\max\{e_d+L_q\omega_e|s_q|,e_q+L_d\omega_e|s_d|\} \tag{12}$$

III. Estimation of Rotational Speed and Rotor Position

Through the new sliding mode observer proposed in this paper, can be obtained. From (9), it can be seen that the EMF in the d-q rotating frame contains the electric angular velocity information, so the electric angular velocity can be expressed as

$$\omega_e=\frac{e_q}{\psi_f} \tag{13}$$

Furthermore, the position of the rotor can be obtained by integrating the angular velocity with time. However, in the actual operation of the motor, affected by temperature and other factors, the rotor flux is not a fixed value. Therefore, the electric angular velocity and rotor position calculated by this method are not accurate, which seriously affects the control performance of the whole motor system. In order to avoid the influence of rotor flux change on position estimation, it is necessary to design a scheme with good anti-disturbance characteristics.

The induced EMF of PMSM in d-q estimated frame can be written as

$$\begin{cases}e_d=e\sin(\hat{\theta}_e-\theta_e)\\e_q=e\cos(\hat{\theta}_e-\theta_e)\end{cases} \tag{14}$$

where $e=\sqrt{e_d^2+e_q^2}$, $\hat{\theta}_e$ is the estimated rotor position angle, θ_e is the actual rotor position.

When the estimated rotor position angle is equal to the actual rotor position angle, the d-axis induced EMF is equal to 0. Therefore, the accuracy of speed and position estimation can be improved by PLL to avoid the influence of harmonic components in observed induced EMF. Fig. 2 shows the block diagram of PLL.

According to Fig. 2, the closed-loop transfer function of the system is expressed as

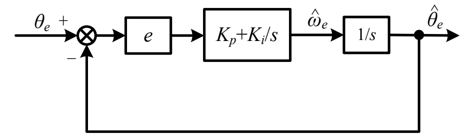

Fig. 2. Block diagram of PLL.

$$G(s)=\frac{\hat{\theta}_e(s)}{\theta_e(s)}=\frac{eK_ps+eK_i}{s^2+eK_ps+eK_i} \tag{15}$$

where K_p, K_i are the proportional and integral gain, respectively.

According to the standard form of the closed-loop transfer function of the second-order system, the parameter of PI regulator can be calculated as

$$\begin{cases}K_p=\dfrac{\sqrt{2}\omega_n}{e}\\K_i=\dfrac{\omega_n^2}{e}\end{cases} \tag{16}$$

where ω_n is the expected closed-loop bandwidth of the system, T is the time constant.

The new sensorless system proposed in this paper is shown in Fig. 3. Firstly, the induced EMF of d and q axes can be obtained by the new sliding mode observer after the voltage and current of d and q axes pass through low-pass filter and zero order state holder respectively. Then, the speed and position can be estimated by PLL.

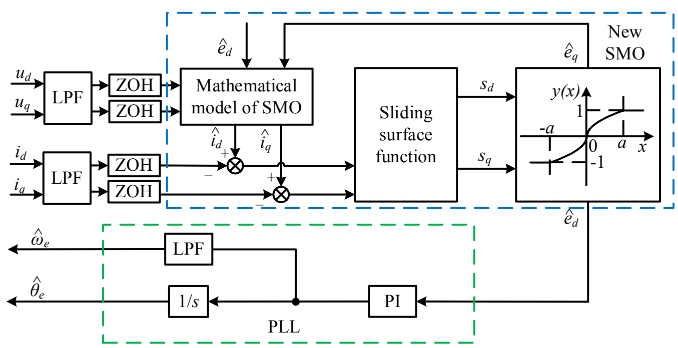

Fig. 3. Block diagram of the proposed sensorlesss system.

IV. Single Resistance Current Reconstruction

In this paper, the sample resistor R_s in series on the DC bus. The three-phase current is reconstructed by sampling bus current combining the current switching state. Space Vector Pulse Width Modulation (SVPWM) is adopted in this paper. The relationship between bus current and three-phase current under basic voltage vector is shown in Table I.

In a PWM cycle, when two basic voltage vectors act, sample the bus current. Then, according to the relationship between bus current and three-phase current in Table I obtain two-phase current, and use $i_a+i_b+i_c=0$ obtain residual phase current. Finally, three-phase current reconstruction is realized.

In practical application, in order to obtain accurate current information, it is necessary to meet the limit of the minimum sampling window.

Time T_{min} corresponding to the minimum sampling window can be expressed as

TABLE I
BASIC VOLTAGE VECTOR AND SAMPLING PHASE CURRENT

Sector	Basic voltage vector	Relationship between bus current and three-phase current
1	100	i_a
	110	$-i_c$
2	110	$-i_c$
	010	i_b
3	010	i_b
	011	$-i_a$
4	011	$-i_a$
	001	i_c
5	001	i_c
	101	$-i_b$
6	101	$-i_b$
	100	i_a

$$T_{\min} = T_d + T_{AD} + T_{set} \tag{17}$$

where T_d is dead time, T_{AD} is A-D conversion time, T_{set} is bus current stabilization time.

In order to meet the minimum sampling window limit, it is necessary to compensate the sector transition area and low-voltage modulation area existing in each sector when using SVPWM. The compensation method adopted in this paper is phase shifting, which increases the vector action time in the sampling area and reduces the vector action time in the non sampling area to ensure that the resultant voltage vector remains unchanged. The sector transition area and low-voltage modulation area are shown in Fig. 4, and the compensation for the sector transition area and low-voltage modulation area is shown in Fig. 5.

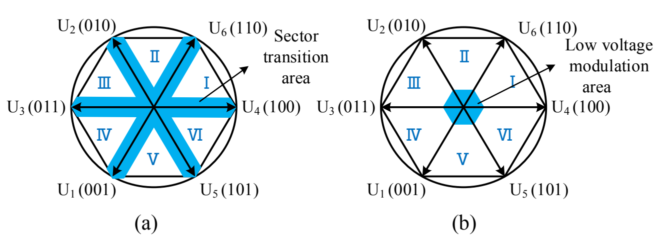

Fig. 4. Non-observation area. (a) Sector transition area. (b) Low voltage modulation area.

The red region vector (101) in Fig. 5(c) is the additional vector generated during the phase shifting of the green region in Fig. 5(a), and the red region vector (101) and purple region vector (001) in Fig. 5(d) are the additional vectors generated during the phase shifting of the blue region and green region in Fig. 5(a), respectively. After phase shifting, the green and blue areas in Fig. 5(c) and Fig. 5(d) are the sampling areas, which ensures the effectiveness and accuracy of sampling.

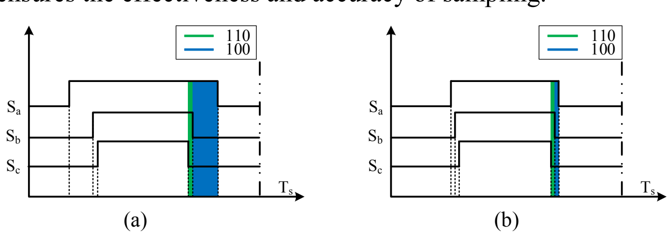

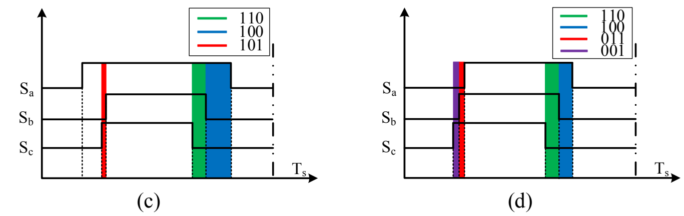

Fig. 5. Vector of Non-observation area and compensation method. (a) Vector of sector transition area. (b) Vector of low voltage modulation area. (c) Compensation of sector transition area. (d) Compensation of low voltage modulation area.

V. SIMULATION ANALYSIS

In order to verify the effectiveness of the new sliding mode observer and single resistor current reconstruction scheme proposed in this paper, based on the permanent magnet synchronous motor shown in Table Ⅱ, a PMSM sensorless vector control system simulation model as shown in Fig. 6 was built in MATLAB/Simulink, and simulation analysis and verification were carried out. The new sliding mode observer and the single resistor current reconstruction are used in proposed scheme together in this paper.

TABLE II
PARAMETER OF PMSM

Parameter	Value
Rated power/kW	1.3
Rated current/A	5
Rated speed/(r/min)	1500
Rated torque/(N·m)	8.34
Pole-pairs	5
Stator resistance/Ω	2
d, q axis inductance/mH	9.55
Flux/Wb	0.18

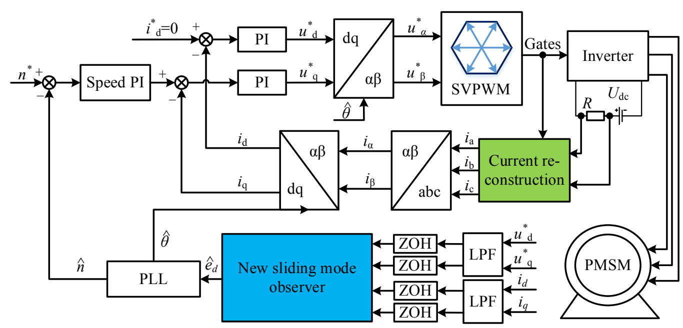

Fig. 6. Diagram of sensorless vector control of PMSM.

Fig. 7 shows the speed, estimated position and reconstructed current waveform of the motor system from start-up to rated speed using traditional and new sliding mode observers, respectively. The simulation results show that the speed chattering in the traditional scheme shown in Fig. 7(a) is larger, the current fluctuates obviously under no-load and rated load, and there is a certain error between the estimated position and the actual position. However, after using the new sliding mode observer in Fig. 7(b), the speed almost has no chattering, the current has almost no fluctuation under no-load and rated load, and the position estimation error is further reduced. The result in Fig. 7 fully confirms the chattering suppression effect of the proposed sliding mode observer.

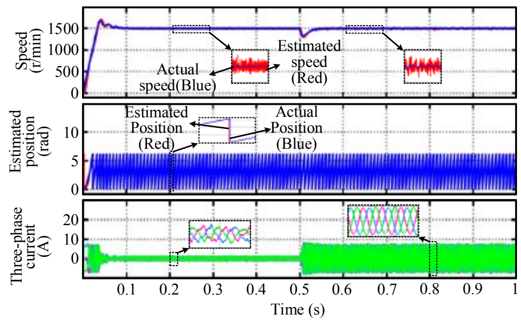

(a)

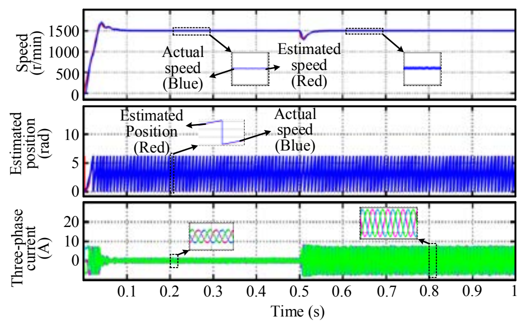

(b)

Fig. 7. Simulation results of motor at rated speed. (a) Traditional sliding mode observer. (b) New sliding mode observer.

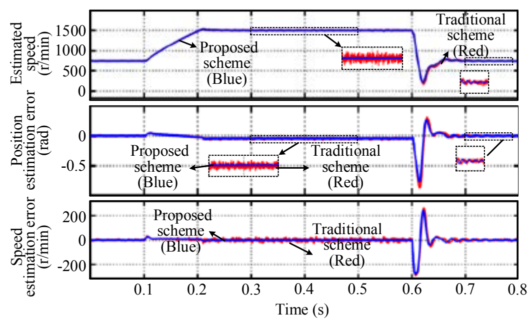

Fig. 8. Simulation results of speed mutation.

Fig. 8 shows the comparative simulation results of the sudden change of motor speed. The motor speed is suddenly increased from 750r/min to 1500r/min at 0.1s and then from 1500r/min to 750r/min at 0.6s. The comparison shows that the position estimation error and speed estimation error of the traditional scheme are significantly larger than those of the proposed scheme in the process of sudden acceleration and deceleration of the motor. Thus, the new sliding mode observer proposed in this paper has better dynamic performance and buffeting suppression effect.

Fig. 9 shows the simulation comparison of the speed, speed estimation error and position estimation error of the motor in the case of sudden load change between the traditional and the proposed scheme. The motor suddenly increases the rated load at 0.2s and decreases to no load at 0.6s. Compared with the proposed scheme, the speed estimation error and position estimation error of the traditional scheme are obviously increased, and the chattering of the traditional scheme is serious. It can be seen that the stability and dynamic performance of the scheme proposed in this paper have obvious advantages in the case of sudden change of system load.

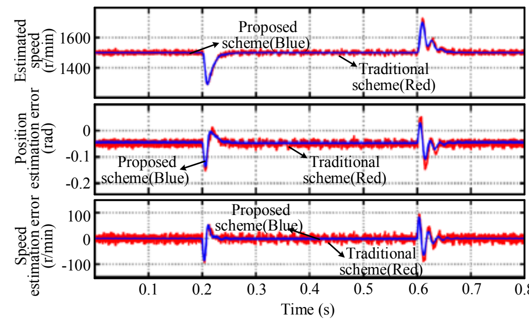

Fig. 9. Simulation results of load mutation.

Fig. 10 shows the actual current, reconstruction current and A-phase current error of the motor under rated speed and rated load. It can be seen from Fig. 10 that the reconstructed three-phase current still has some errors compared with the actual three-phase current in the low-voltage modulation region, but on the whole, the reconstructed three-phase current can meet the requirements of the motor control scheme.

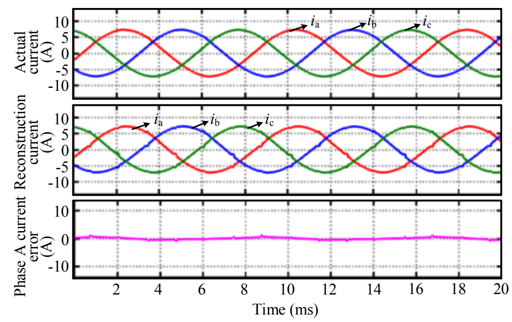

Fig. 10. Simulation results of current reconstruction.

VI. Conclusion

In this paper, a sensorless control scheme of PMSM based on new sliding mode observer and single resistor current reconstruction is proposed. Firstly, a piecewise square root switching function is designed, which makes use of the characteristics of continuity in the boundary layer and saturation outside the boundary layer to effectively restrain the chattering problem of the traditional sliding mode observer. Secondly, a single resistor used to sample bus current for current reconstruction is adopted. By analyzing the relationship among bus current, phase current and switching state, the bus current sampled by resistor is used to reconstruct the three-phase current without current sensor. The sensorless technology based on single resistance current reconstruction proposed in this paper reduces the driving cost, does not need to use mechanical position sensor and current sensor, and increases the reliability of the system. However, the problem of waveform distortion of current reconstruction and the error of position estimation in the non-observation area are worthy of further study and solution.

References

[1] J. Liu, F. Xiao, Y. Shen, et al, “Position-sensorless control technology of permanent-magnet synchronous motor-a review,” *Trans. of China Electrotechnical Society*, vol. 32, no. 16, pp. 76-88, Jun. 2017.

[2] G. Wang, M. Valla and J. Solsona, “Position Sensorless Permanent Magnet Synchronous Machine Drives—A Review,” *IEEE Trans. Ind*

Electron, vol. 67, no. 7, pp. 5830-5842, July 2020.

[3] X. Song, J. Fang, B. Han and S. Zheng, "Adaptive Compensation Method for High-Speed Surface PMSM Sensorless Drives of EMF-Based Position Estimation Error," *IEEE Trans. Power Electron*, vol. 31, no. 2, pp. 1438-1449, Feb. 2016.

[4] J. Su, T. Li, G. Yang, "Chattering Phenomenon Analysis and Suppression of Sliding Mode Observer in PMSM Sensorless Control," *Trans. of China Electrotechnical Society*, vol. 24, no. 8, pp. 58-64, Aug. 2009.

[5] H. Wang, F. Xiao, W. Ma, et al, "Sensorless control of PMSG based on sliding mode observer and software phase locked-loop," *Electric Machines and Control*, vol. 15, no. 1, pp. 49-54, Jan 2011.

[6] Z. Qiao, T. Shi, Y. Wang, Y. Yan, C. Xia and X. He, "New Sliding-Mode Observer for Position Sensorless Control of Permanent-Magnet Synchronous Motor," *IEEE Trans. Ind Electron*, vol. 60, no. 2, pp. 710-719, Feb. 2013.

[7] L. Zhang, H. Li, P. Song, et al, "Sensorless Vector Control Using a New Sliding Mode Observer for Permanent Magnet Synchronous Motor Speed Control System," *Trans. of China Electrotechnical Society*, vol. 34, no. 1, pp. 70-78, Jun. 2019.

[8] D. Liang, J. Li and R. Qu, "Sensorless Control of Permanent Magnet Synchronous Machine Based on Second-Order Sliding-Mode Observer With Online Resistance Estimation," *IEEE Trans. Ind Appl*, vol. 53, no. 4, pp. 3672-3682, July-Aug. 2017.

[9] J. Liu, F. Xiao, Z. Mai, et al, "Hybrid Position-Sensorless Control Scheme for PMSM Based on Combination of IF Control and Sliding Mode Observer," *Trans. of China Electrotechnical Society*, vol. 33, no. 4, pp. 919-929, Dec. 2018.

[10] X. Lu, H. Lin, Y. Feng, et al, "Soft Switching Sliding Mode Observer for PMSM Sensorless Control," *Trans. of China Electrotechnical Society*, vol. 30, no. 2, pp. 106-113, Jan. 2015.

[11] D. Lü, Z. Li, "Improved sliding mode observer control of surface mounted permanent magnet synchronous motor," *Electric Machines and Control*, vol. 25, no. 10, pp. 58-66, May. 2021.

[12] C. Gong, Y. Hu, J. Gao, Y. Wang and L. Yan, "An Improved Delay-Suppressed Sliding-Mode Observer for Sensorless Vector-Controlled PMSM," *IEEE Trans. Ind Electron*, vol. 67, no. 7, pp. 5913-5923, July. 2020.

[13] Y. Zhang, J. Wu, H. Wei, et al, "Discrete Variable Gain Super-Twisting Sliding Mode Observer for Permanent Magnet Synchronous Motor," *Trans. of China Electrotechnical Society*, vol. 33, no. 21, pp. 4962-4970, Nov. 2018.

[14] L. Woo-Cheol, L. Taeck-Kie and H. Dong-Seok, "Comparison of single-sensor current control in the DC link for three-phase voltage-source PWM converters," *IEEE Trans. Ind Electron*, vol. 48, no. 3, pp. 491-505, June. 2001.

[15] H. Wei, Y. Lu, T. Jiang, et al, "Single Resistor Sampling Reconstruction of Permanent Magnet Synchronous Motor Considering Non-Observation Area Compensation," *Trans. of China Electrotechnical Society*, vol. 33, no. 12, pp. 2695-2702, Apr. 2018.

[16] W. Wang, H. Yan, J. Zou, et al, "Phase Current Re-construction Strategy of PMSM Under Overmodulation Mode Based on a Hybrid Space Vector Pulse Width Modulation Technique," *Proceedings of the CSEE*, vol. 41, no. 17, pp. 6050-6060, Dec. 2021.

Qingguo Sun (Member, IEEE) received the B.S. degree in electrical engineering from Qingdao University, Qingdao, China, in 2014, and the Ph.D. degree from the College of Electrical Engineering, Zhejiang University, Hangzhou, China, in 2019. He is currently a lecturer with the School of Electrical Engineering, Hebei University of Technology, Tianjin, China. He has authored more than 30 technical articles and 10 issued/published invention patents.

His research interests include motor control, motor design, and high-efficiency power converters.

Xiaolei Zhu received the B.S. degrees in electrical engineering from Tiangong University, Tianjin, China, in 2020 and now he is studying for the M.S. degree in the School of Electrical Engineering of Hebei University of Technology.

His research interests include the control of permanent magnet motor.

Feng Niu (Member, IEEE) was born in Hebei, China, in 1986. He received the B.S. and Ph.D. degress in electrical engineering from the Hebei University of Technology, Tianjin, China, in 2009 and 2015, respectively. From 2016 to 2018, he was a Postdoctoral Research Fellow with the College of Electrical Engineering, Zhejiang University, Hangzhou, China. He is currently a Professor with the School of Electrical Engineering, Hebei University of Technology. He has authored or coauthored more than 40 techinal articles.

His current research interests include motor system and intelligent electrical equipment.